ASTRONOMY & ASTROPHYSICS
SUPPLEMENT SERIES

FEBRUARY II **2000**, PAGE 41

Astron. Astrophys. Suppl. Ser. **142**, 41–57 (2000)

A ROSAT PSPC catalogue of X-ray sources in the SMC region⋆

F. Haberl[1], **M.D. Filipović**[1,2,3], **W. Pietsch**[1], **and P. Kahabka**[4,5]

[1] Max–Planck–Institut für extraterrestrische Physik, Giessenbachstrasse, 85748 Garching, Germany
[2] University of Western Sydney Nepean, P.O. Box 10, Kingswood, NSW 2747, Australia
[3] Australia Telescope National Facility, CSIRO, P.O. Box 76, Epping, NSW 2121, Australia
[4] Astronomical Institute, University of Amsterdam, Kruislaan 403, NL-1098 SJ Amsterdam, The Netherlands
[5] Center for High Energy Astrophysics, University of Amsterdam, Kruislaan 403, NL-1098 SJ Amsterdam, The Netherlands

Received October 8; accepted November 19, 1999

Abstract. We present a catalogue of 517 discrete X-ray sources in a $6°\times6°$ field covering the Small Magellanic Cloud (SMC). The catalogue was derived from the pointed ROSAT PSPC observations performed between October 1991 and May 1994 and is complementary to the Large Magellanic Cloud (LMC) catalogue published by Haberl & Pietsch (1999). We followed the same identification scheme and used, among other information, X-ray hardness ratios and spatial extent to classify unknown sources as candidates for active galactic nuclei (AGN), foreground stars, supernova remnants (SNRs), supersoft sources (SSSs) and X-ray binaries. For 158 sources a likely source type is given, from which 46 sources are suggested as background AGN (including candidates resulting from a comparison of X-ray and radio images). Nearly all of the X-ray binaries known in the SMC were detected in ROSAT PSPC observations; most of them with luminosities below 10^{36} erg s^{-1} suggesting that the fraction of high luminosity X-ray binary systems in the Magellanic Clouds (MCs) is not significantly larger than in our galaxy. Seventeen X-ray sources are associated with SNRs found in earlier work and we suggest here two additional extended sources as SNR candidates. Three very soft sources are newly classified as SSSs from which one is identified with the symbiotic star LIN 358 in the SMC.

Key words: catalogues — ISM: supernova remnants — galaxies: magellanic clouds — galaxies: stellar content — X-rays: galaxies — X-rays: stars

Send offprint requests to: F. Haberl
e-mail: fwh@mpe.mpg.de

⋆ Table 2 is only available in electronic form at CDS via anonymous ftp to cdsarc.u-strasbg.fr (130.79.128.5) or via http://cdsweb.u-strasbg.fr/Abstract.html

1. Introduction

The most comprehensive X-ray studies of the MCs before the launch of ROSAT were performed using the imaging instruments on the Einstein satellite. After a final unified analysis of the IPC data, Wang et al. (1991) and Wang & Wu (1992, hereafter WW92) published catalogues of 105 and 70 discrete X-ray sources in the LMC and SMC regions, respectively. With ROSAT (Trümper 1982) the amount of high angular resolution X-ray data from the MCs increased considerably. Many pointed observations from various scientific programs, in particular using the PSPC imaging detector ($0.1 - 2.4$ keV; Pfeffermann et al. 1986), are available to completly survey both Clouds. Haberl & Pietsch (1999, hereafter HP99) analyzed more than 200 PSPC pointed observations covering 59 square degrees in the field towards the LMC. They compiled a catalogue of 758 point and point-like X-ray sources and used the properties of identified sources to classify nearly 100 sources as new candidates for SNRs, X-ray binaries, SSSs, foreground stars and background AGN.

Kahabka & Pietsch (1996) conducted a PSPC survey of the SMC covering 9 square degrees and Kahabka et al. (1999, hereafter KPFH99) published a first ROSAT PSPC catalogue with 248 X-ray sources. The number of PSPC observations finally available in the ROSAT archive is twice of that used by KPFH99. We therefore analyzed the whole set of PSPC pointings towards the SMC to derive a complete catalogue of PSPC sources in the SMC region as was provided by HP99 for the LMC. To obtain this new complementary catalogue the analysis was done the same way as in HP99 (Sect. 2). In Sect. 3 we present the ROSAT PSPC catalogue of SMC sources together with a classification based on various properties.

2. ROSAT PSPC observations and analysis

ROSAT performed 31 pointed PSPC observations with at least 200 s of exposure in a $6^\circ \times 6^\circ$ area centered on the position RA = $01^h\ 00^m\ 00^s$ Dec = $-73^\circ\ 30'\ 00''$ in the SMC between 1990 and 1994. Most of the observations (summarized in Table 1) had exposures between 5 ks and 20 ks and in one case reached 64.6 ks (centered on CF Tuc).

An X-ray image of the SMC produced from merged ROSAT PSPC data in the energy band $0.5 - 2.0$ keV is shown in Fig. 1. The image is exposure corrected but not background subtracted and covers an exposed area of ∼18 square degrees. Time intervals with a total count rate of more than 15 cts s^{-1} were excluded to keep the background at the lowest possible level and uniform in the image. The image was binned to 1536×1536 pixels of $15'' \times 15''$ size and smoothed with an intensity dependent Gaussian filter before the exposure correction (stronger smoothing at the low intensity levels and no smoothing above 15 counts per pixel to avoid smearing out the stronger point sources). The still visible blurring is caused by the telescope when sources are observed far off-axis (see the sources at the rim of the exposures). For this reason conclusions on possible diffuse emission in the SMC require a more careful quantitative study beyond the scope of this paper. A wealth of X-ray sources is detected in the ROSAT PSPC data with most sources concentrated in the northern part of the SMC. The combination of three images in the energy bands $0.1 - 0.4$ keV, $0.5 - 0.9$ keV and $0.9 - 2.0$ keV into a red-green-blue (RGB) image is shown in Fig. 2. The colours illustrate the different X-ray spectra of various source types. Sources with soft X-ray spectra (high intensities in the "red" $0.1 - 0.4$ keV band) like foreground stars and in particular SSSs appear in orange/red. SNRs are characterized by harder spectra and green to blue colours. Absorbed AGN and X-ray binaries show the hardest X-ray spectra and blue colours in the RGB image.

We used the EXSAS software package (Zimmermann et al. 1994) for the analysis of the individual pointings and followed the same lines as in HP99 for the LMC. However, the 31 SMC observations covered 16 different fields and pointings in the same direction were merged to gain sensitivity. In these cases both merged and individual images were run through the source detection procedure. After the final visual inspection of the source list a catalogue of 517 point-like and weakly extended sources was obtained with source properties as given in the LMC catalogue of HP99. Both catalogues comprise complementary lists of sources detected with the ROSAT PSPC in the fields of the MCs.

Table 1. ROSAT PSPC observations of the SMC region

ID	Exp. s	Date begin	Date end	RA (J2000.0)	Dec (J2000.0)
201094p	64636	921002	921111	00 50 48.00	−74 46 48.0
300369p	5640	930928	931101	01 22 55.02	−75 21 00.0
300369p-1	213	940401	940401	01 22 55.02	−75 21 00.0
400022p	16634	911007	911008	01 17 04.08	−73 26 24.0
400022p-1	8985	920930	921002	01 17 04.08	−73 26 24.0
400022p-2	11864	930603	930604	01 17 04.08	−73 26 24.0
400149p	6281	920428	920603	00 37 19.02	−72 14 24.0
400299p	5121	930410	930424	00 37 19.02	−72 14 24.0
400299p-1	1677	931002	931009	00 37 19.02	−72 14 24.0
400299p-2	2311	940503	940505	00 37 19.02	−72 14 24.0
400300p	5214	930329	930330	00 58 33.06	−71 36 00.0
400300p-1	7199	931001	931009	00 58 33.06	−71 36 00.0
400300p-2	4111	940505	940505	00 58 33.06	−71 36 00.0
500142p	4909	930512	930513	01 04 02.04	−72 01 48.0
500249p	19262	931105	931109	00 46 40.08	−73 12 36.0
500250p	20860	931014	931029	01 04 38.04	−72 05 23.5
500251p	2093	931130	931130	00 51 19.02	−73 24 00.0
600195p-0	16644	911008	911103	00 58 12.00	−72 16 48.0
600195p-1	9443	920417	920427	00 58 12.00	−72 16 48.0
600196p-0	1303	911009	911102	00 50 45.06	−73 13 48.0
600196p-1	22223	920415	920425	00 50 45.06	−73 13 48.0
600197p	21494	911016	911019	01 13 24.00	−72 49 12.0
600452p	14207	930410	930425	01 05 55.02	−72 33 35.5
600452p-1	16663	931001	931014	01 05 55.02	−72 33 35.5
600453p	17593	930509	930512	00 54 28.08	−72 45 36.0
600454p	9727	921205	921208	00 42 55.02	−73 38 24.0
600454p-1	8299	930405	930426	00 42 55.02	−73 38 24.0
600455p	3561	921206	921206	01 01 16.08	−71 49 12.0
600455p-1	1721	930416	930422	01 01 16.08	−71 49 12.0
600455p-2	4595	931007	931010	01 01 16.08	−71 49 12.0
600455p-3	4129	940504	940505	01 01 16.08	−71 49 12.0

3. The catalogue of discrete X-ray sources

Table 2 with the full SMC catalogue is available electronically and contains the following information for each X-ray source: (1) source number, (2) likelihood of existence (maximum value from the five detection energy bands) ML_{exi}, (3) vignetting corrected net exposure, (4) and (5) source coordinates RA and Dec (J2000.0) derived from observation and energy band with smallest position error, (6) statistical 90% confidence error on the X-ray position with an additioanl systematic uncertainty of about $7''$, (7) PSPC $0.1-2.4$ keV count rate and error, (8) and (9) hardness ratios (defined as HR1 = (H − S)/(S+H) and HR2 = (H2 − H1)/(H1+H2) where S, H, H1 and H2 denote count rates in the $0.1 - 0.4$ keV, $0.5 - 2.0$ keV, $0.5 - 0.9$ keV and $0.9 - 2.0$ keV bands, respectively; not calculated in cases where not all required count rates are available), (10) source extent from same detection as source position, (11) likelihood for the extent, (12) ROSAT observation identifier (a "+" at the end marks merged observations), (13) off-axis angle, (14) distance to detector window support structure or detector rim (WSS), (15) number of nearest (within $60''$) source in KPFH99 (see Sect. 3.1) and (16) remark (cf. Table 1 in HP99). We note here that the count rates given in KPFH99 and here can considerably differ for sources repeatedly covered by PSPC observations. Since the main goal of this work is to identify sources, we selected the detection with smallest error on the X-ray

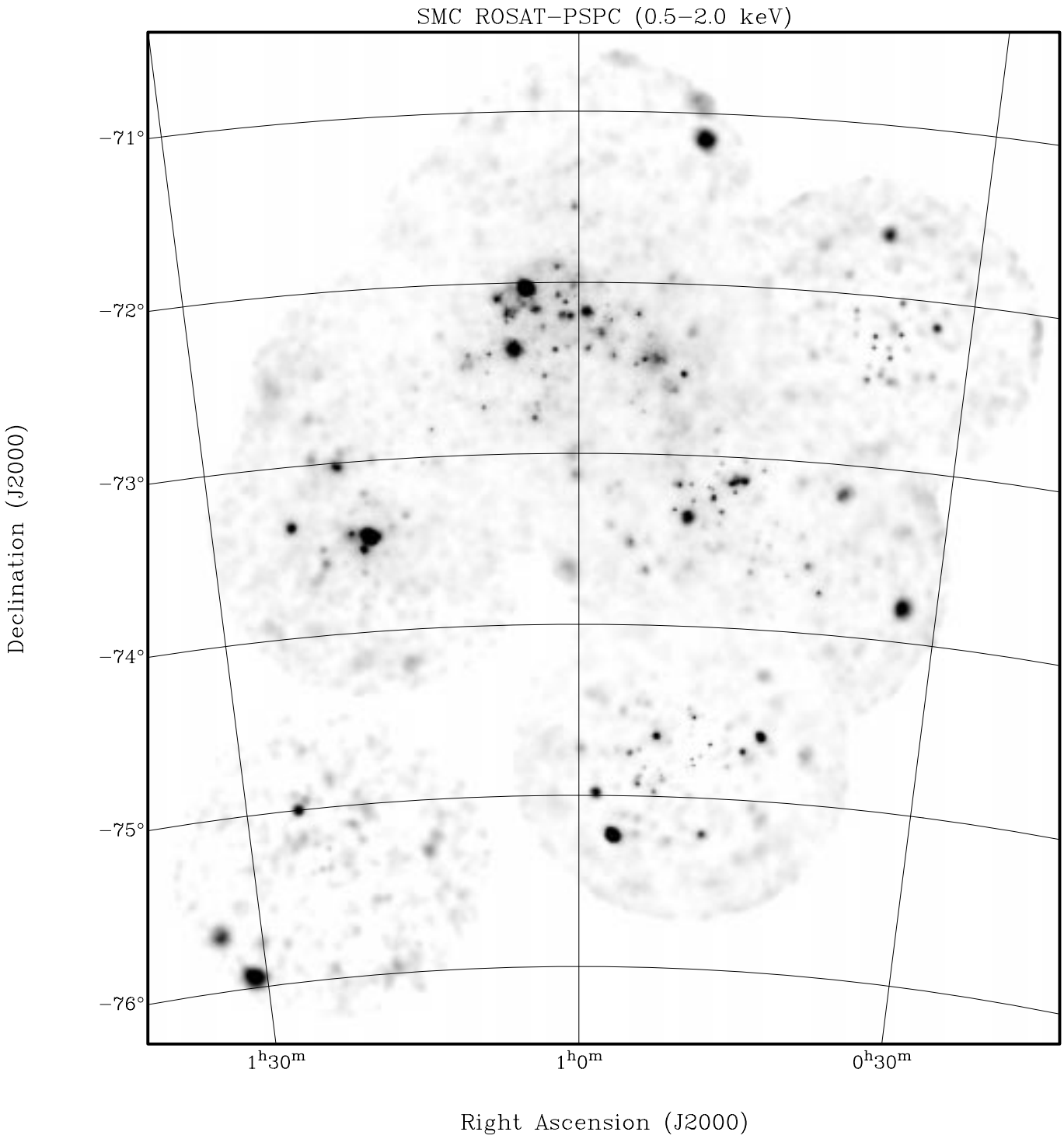

Fig. 1. Exposure corrected $0.5 - 2.0$ keV image of the combined ROSAT PSPC observations in the SMC region

position which may result from a different PSPC observation not used by KPFH99.

The spatial distribution of the 517 PSPC sources in the catalogue is shown in Fig. 3. Haberl & Pietsch (1999) have used the LMC catalogue to identify known sources and classify unknown sources according to the properties of the identified samples. Again we follow the same procedures for the SMC region.

3.1. Comparison with previous X-ray surveys

In Table 3 we summarize 50 PSPC sources which have an Einstein IPC counterpart (from Tables 2A and B in WW92) within 90″. The IPC and PSPC count rates are compared in Fig. 4 where the sources identified with a SNR are marked with a circle. A linear fit to the SNR count rates gives a mean conversion factor of 2.8 for IPC

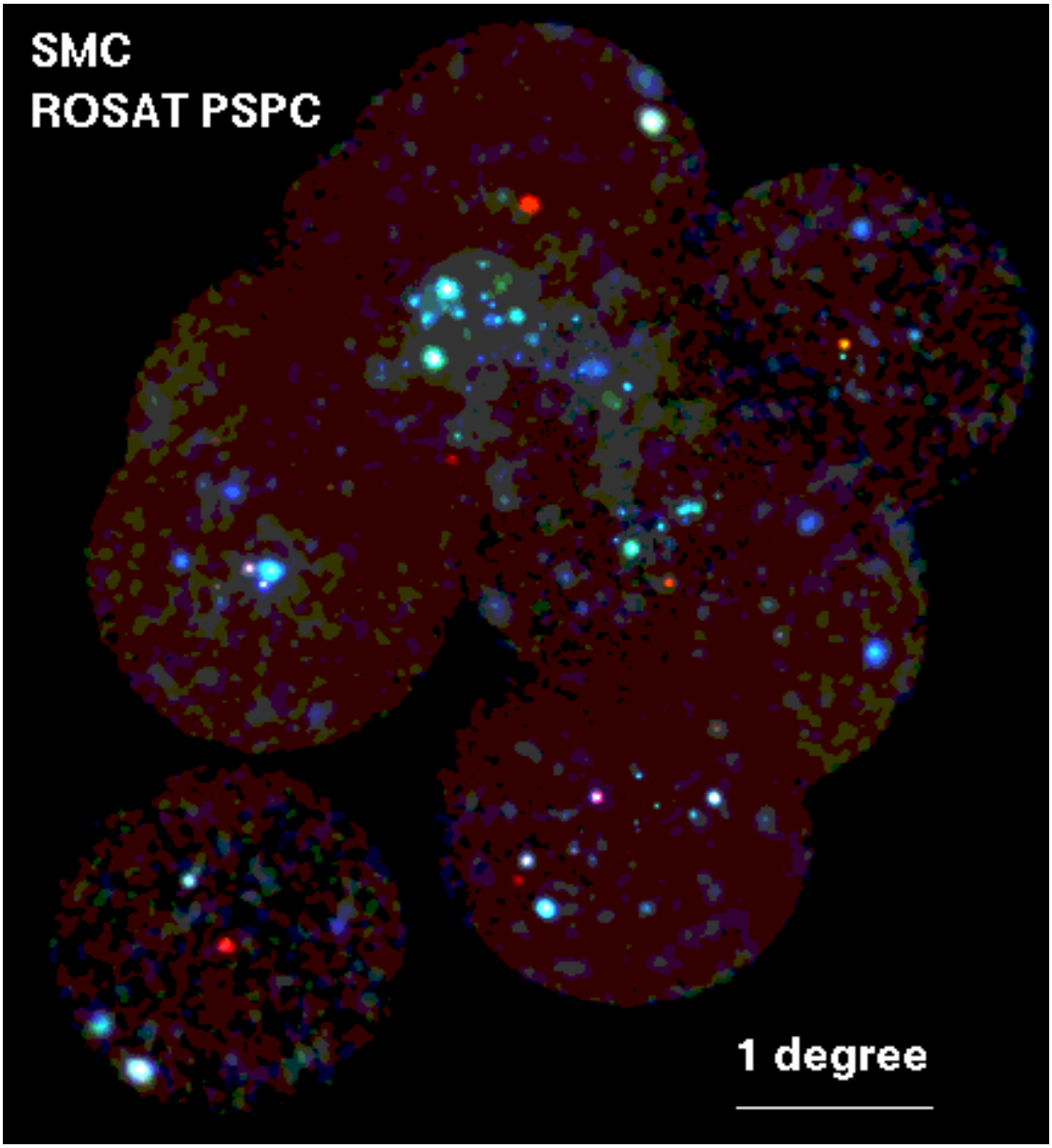

Fig. 2. PSPC images in the energy bands $0.1 - 0.4$ keV, $0.5 - 0.9$ keV and $0.9 - 2.0$ keV combined into a red-green-blue (RGB) colour coded image

to PSPC count rates, somewhat smaller than found in the LMC which is compatible with a slightly higher foreground absorption. The high mass X-ray binary (HMXB) pulsar SMC X-1 and the RSCVn type foreground star HD 5303 were significantly brighter during the ROSAT observations (because the best source detection with smallest position error enters the catalogue, detections during bright source state are preferentially selected) while the pulsar RX J0051.8-7231 probably associated with the IPC source 0050.1-7248 was bright during the Einstein observations. The unidentified ROSAT source 320 may be associated with 0101.3-7300 (a relatively large correlation distance leaves some doubt) in which case the classification as foreground star suggests a flare during the IPC observation.

A correlation of the PSPC catalogue from the pointed observations with the Bright Source Catalogue (BSC) of the ROSAT all-sky survey (Voges et al. 1996, 1999) yields 16 sources within a distance of $60''$ which are summarized in Table 4. Strong variability between survey and pointed observations was found for the two brightest sources of this sample (SMC X-1 and HD 5303) and for the SSS RXJ 0048.4-7332 which was more than a factor 20 fainter during the pointing with identifier 500251p than during survey. However, during other pointings RXJ 0048.4-7332

Table 2. Excerpt of the catalogue of 517 ROSAT PSPC sources from a 6°×6° field centered on the SMC

1	2	3	4	5	6	7	8	9	10	11
No	ML_{exi}	Exp. [s]	RA (J2000.0)	Dec	r_{90} [″]	Count Rate [cts s^{-1}]	HR1	HR2	Extent [″]	ML_{ext}
49	12.2	15341	01 02 49.5	−71 37 09	42.6	3.41e-03 ± 4.4e-03	1.00 ± 0.84	−1.00 ± 1.69	0.0	0.0
50	47.1	14862	00 55 47.3	−71 38 03	10.0	4.90e-03 ± 7.4e-04	−0.22 ± 0.15	−0.21 ± 0.22	0.0	0.0
51	25.7	15176	00 59 41.7	−71 38 15	14.5	2.94e-03 ± 6.1e-04	−1.00 ± 0.12		0.0	0.0
52	326.6	9397	00 36 56.9	−71 38 15	17.5	3.86e-02 ± 2.8e-03	1.00 ± 0.25	0.38 ± 0.06	3.4	19.1
53	21360.4	3470	00 59 11.3	−71 38 45	2.8	8.38 ± 5.0e-02	0.48 ± 0.01	0.17 ± 0.01	1.1	14.5

12	13	14	15	16
ROR	δ [′]	d_{rib} [FWHM]	KPFH99	Remark
500250p	29	1.3	0	AGN? 13 cm
400300p+	13	6.0	109	fg Star F5/F6V, HD 5572 (SIM)
400300p+	6	20.6	141	SSS? RXJ0059.6-7138, PN LIN357 (KPFH99)
400299p+	36	1.8	19	AGN? [hard] [nonstar] Radio SMC B0034-7155 (FJW97) 13 cm jets
500142p	32	4.3	0	HMXB Be/X RXJ0059.2-7138, soft pulsar (H94, SC96)

was detected with count rates similar to the survey intensity (see Kahabka et al. 1994).

The first SMC catalogue based on ROSAT PSPC data and published by KPFH99 is less complete than the catalogue presented here mainly due to the limited number of observations and the more restricted field of view (45′ vs. 52′) used for the analysis. A correlation of the two catalogues shows that 209 sources have a counterpart within 60″. For these the source number from KPFH99 is given in Table 2. The 39 sources of KPFH99 without counterpart in the new catalogue are summarized in Table 5. KPFH99 marked 15 of these with "D" as probable artifacts close to the WSS and we confirm that they are not real. Four other sources with relatively high likelihood are probably also false detections: source 223 in KPFH99 is the most extended one and not visible on the PSPC images; sources 75, 165 and 185 are near the WSS. Two sources (25, 186) are also near the WSS but may be real. Another 17 sources have likelihood values smaller than 15, close to our acceptance threshold and a slightly different background map used in the analysis is probably the reason why they are not detected in our analysis. Source 60 may be resolved into two X-ray sources (413 and 419 in the present catalogue) in an observation which was not used by KPFH99 but has source 60 closer to its field center. Source 413 coincides with a known SNR showing radio emission. Inspecting the ATCA $\lambda = 13$ cm image (see below) shows that the radio emission is associated with source 413 suggesting that 419 is a separate source.

3.2. Source identification and classification

Source identifications were mainly obtained by cross-correlation of the SMC catalogue with the SIMBAD data base operated at CDS. The derived samples of known X-ray sources show identical properties to those of the LMC and therefore we used similar classification criteria as for the LMC sources (Table 6; cf. Table 3 of HP99). As only exception, the selection for SSS was expanded to HR1+EHR1 < -0.70 which includes all sources with HR2+EHR2 < -0.70.

To select objects with high X-ray to optical flux ratio we enlarged the f_x/f_{opt} classification used for the LMC. By using the optically brightest object in the error circle (to be conservative the 90% confidence error including the systematic error was multiplied by 1.5) a lower limit for the X-ray to optical flux ratio is derived. For this purpose optical R and B magnitudes were taken from the USNO-A1.0 catalogue produced by the US Naval Observatory. Finally selecting objects with $\log(f_x/f_B)$ greater than 0 excludes foreground stars and we classified these as [nonstar.] Sources of this type in the observed regions outside the main regions of the SMC are candidates for background sources and if south of −74° 30′ were in addition classified as [AGN]. However, we note that the H I emission of the SMC (Stanimirovic et al. 1999) extends that far south and finding X-ray binaries there is not completely ruled out.

Figures 5, 6 and 7 illustrate the selection criteria used for source extent, hardness ratios and X-ray to optical flux ratio. As in the LMC, the identified well known SNRs show the highest extent likelihoods and the two classified SNR candidates (mainly from hardness ratio selection) are found with significant X-ray extent. Also similar to the LMC the different source types separate in different regions of the HR diagram (Fig. 6) which can be divided into the same areas as in the LMC case. There is one object (source 380) with hardness ratios compatible to that

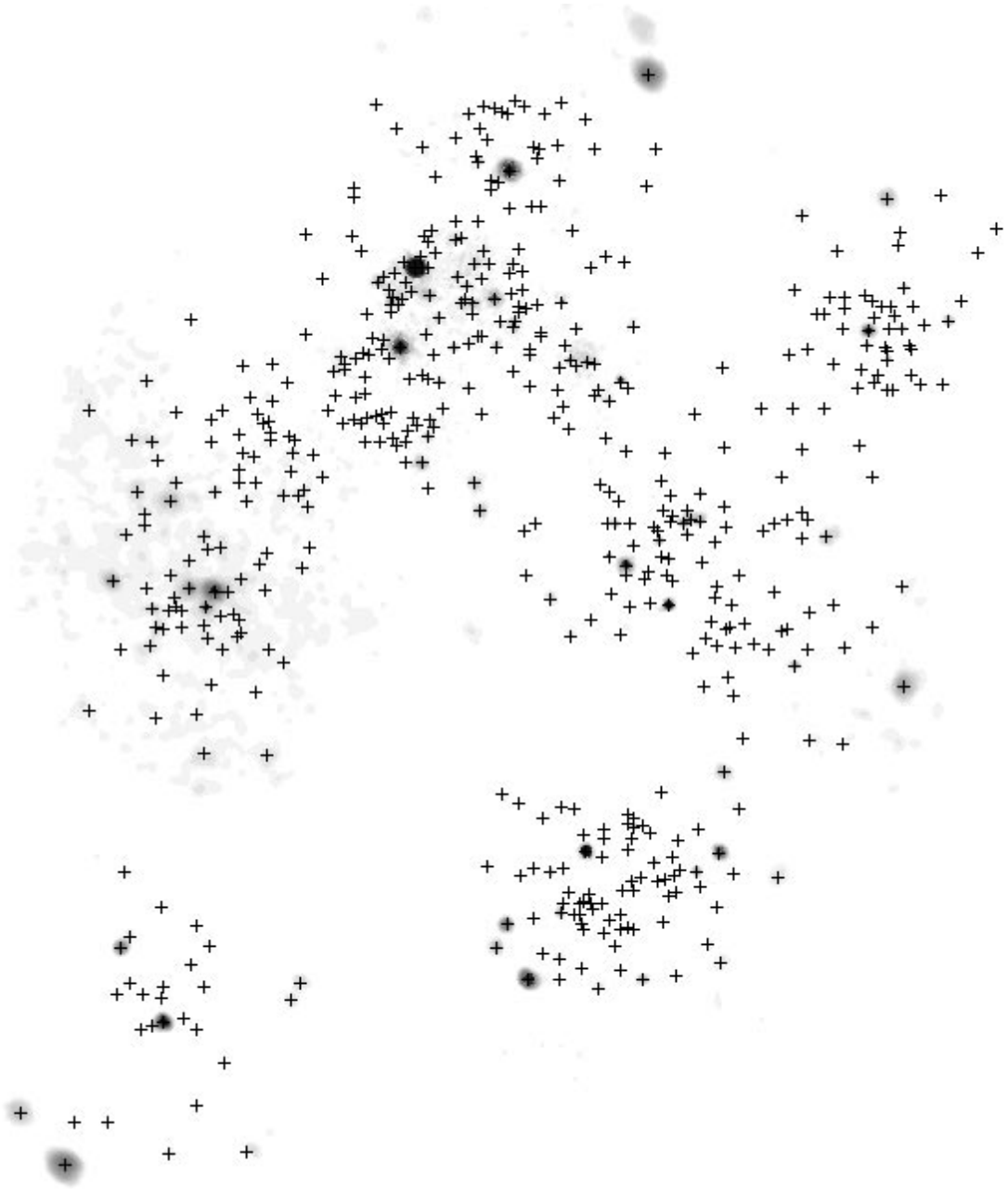

Fig. 3. Distribution of the 517 X-ray sources detected with the ROSAT PSPC. The source positions are plotted on a weak grey scale image ($0.1 - 2.4$ keV) similar to Fig. 1 for orientation

of foreground stars which was classified as [nonstar] due to its high X-ray to optical flux ratio. A nearby radio source suggests the source as AGN candidate. The X-ray binary with HR1 near 0.5 marks the peculiar soft X-ray pulsar (source 53, H94). Foreground stars are well recognized from their hardness ratios and also from their low X-ray to optical flux ratio, i.e. typically $\log(f_{\rm x}/f_{\rm opt}) < -1$ (Fig. 7). Most of the objects with high $f_{\rm x}/f_{\rm opt}$ have errors on HR1 larger than 0.25 and are not shown in (Fig. 7).

Table 7 summarizes the properties of 158 identified and classified sources sorted by source class. The classification (including candidates) is complete for the 44 brightest sources down to a PSPC count rate of 0.02 cts s^{-1}. This sample consists of 27% foreground stars, 16% background objects, 20% high mass X-ray binaries, 16% SNRs, 9% SSSs in the SMC and 9% sources which are probably either AGN or HMXBs. We expect at lower intensity levels less foreground stars but more background AGN.

Table 3. PSPC sources detected with the Einstein IPC

1	2		3	4	5	6	7
No	WW92 No	Name	d [″]	r_{90} [″]	PSPC Count Rate [cts s^{-1}]	IPC Rate [cts s^{-1}]	Remarks
8	23	0049.0-7125	15.5	20.2	2.04e-01 ± 1.1e-02	0.046	fg Star F5V, HD 5028 (WW92)
47	43	0056.8-7152	2.6	1.3	3.68e-01 ± 4.9e-03	0.047	SSS 1E0056.8-7154, PN LIN333 (KP96)
94	32	0051.3-7213	62.2	30.2	1.21e-02 ± 2.1e-03	0.006	
107	51	0102.3-7218	13.4	0.7	2.24 ± 2.1e-02	0.807	SNR 0102-72.3 (WW92,FPW99) 13 cm
114	41	0056.2-7219	58.3	7.9	3.03e-03 ± 5.0e-04	0.002	HMXB? AXJ0058-72.0, pulsar (YK98a)
121	46	0059.8-7220	37.6	7.2	8.93e-03 ± 8.5e-04	0.003	
125	54	0104.5-7222	52.1	3.6	3.36e-02 ± 1.5e-03	0.008	SNR 0104-72.3 (WW92) 13 cm
143	50	0101.5-7225	17.5	3.4	1.54e-02 ± 9.6e-04	0.013	HMXB Be/X SAXJ0103.2-7209, pulsar (ISC98, HS94,CO99)
148	44	0057.7-7226	1.4	3.2	5.73e-02 ± 1.7e-03	0.024	SNR 0057-72.2 (YTK91,WW92) 13 cm
157	36	0053.7-7227	20.9	2.3	2.74e-02 ± 1.2e-03	0.005	AGN? Radio SMC B0053-7227 (FHW98) 13 cm jets
160	53	0103.8-7227	49.0	7.8	1.63e-02 ± 1.0e-03	0.011	[hard] associated with DEM S128? (FHP00)
162	45	0059.1-7227	44.5	2.3	2.67e-02 ± 1.1e-03	0.006	[hard] G star identification in SCC99 unlikely
163	53	0103.8-7227	76.9	6.6	6.86e-03 ± 6.7e-04	0.011	HMXB Be/X AXJ0105-722, pulsar (YK98b, FHP00)
170	40	0055.8-7229	14.2	3.6	5.48e-03 ± 5.4e-04	0.006	[hard] [nonstar]
176	13	0035.3-7230	6.1	1.2	4.40e-01 ± 5.4e-03	0.075	SSS 1E0035.4-7230 (KP96)
185	42	0056.5-7233	80.6	19.0	2.32e-03 ± 4.7e-04	0.007	
194	42	0056.5-7233	26.7	6.5	1.00e-02 ± 7.2e-04	0.007	SNR 0056-72.5 (WW92) 13 cm
217	52	0103.2-7239	54.2	2.1	3.12e-01 ± 4.6e-03	0.056	SNR 0103-72.6 (WW92, CSM97) 13 cm
220	47	0100.1-7240	62.1	8.1	9.98e-03 ± 9.5e-04	0.007	
227	55	0105.4-7240	74.9	14.2	9.32e-04 ± 1.3e-03	0.002	
230	55	0105.4-7240	51.4	2.4	1.20e-02 ± 7.1e-04	0.002	[hard]
232	58	0107.1-7241	23.3	8.6	4.93e-03 ± 5.6e-04	0.004	[hard]
234	39	0055.6-7241	20.5	3.4	8.73e-03 ± 6.7e-04	0.003	
241	35	0053.2-7242	20.5	3.5	3.68e-02 ± 1.5e-03	0.009	HMXB Be/X XTEJ0055-724, pulsar (ML98, SCI98, SCB99, CO99)
242	34	0052.1-7242	33.9	25.7	8.50e-02 ± 4.7e-03	0.008	HMXB? XTEJ0053-724, pulsar (CML98)
252	59	0107.1-7244	67.8	13.7	5.62e-03 ± 1.1e-03	0.006	
265	27	0050.1-7248	26.4	45.8	5.45e-03 ± 1.5e-03	0.016	HMXB Be/X RXJ0051.8-7231, pulsar (WW92, ISA97, SCB99)
279	56	0105.6-7251	20.3	11.1	7.44e-04 ± 1.0e-03	0.007	
285	30	0050.9-7253	50.9	12.7	6.86e-03 ± 8.7e-04	0.012	SNR 0050-72.8 (WW92) 13 cm
295	19	0045.6-7256	54.1	49.8	4.06e-03 ± 5.1e-03	0.006	AGN? Radio SMC B0045-7255 (FHW98) 13 cm
320	48	0101.3-7300	53.7	17.2	3.58e-03 ± 7.9e-04	0.027	[fg Star] GSC 9141.7584
333	31	0051.1-7304	79.2	12.5	1.21e-03 ± 4.0e-04	0.008	
361	72	0102.3-7318	8.6	32.4	4.40e-02 ± 9.6e-03		SSS? RXJ0103.8-7254 (KP96)
379	62	0115.1-7315	21.5	14.0	6.04e-03 ± 8.2e-04	0.005	AGN $z = 0.253$ (TDZ97)
385	66	0118.1-7316	19.5	13.2	3.13e-02 ± 1.6e-03	0.013	Cluster $z = 0.0656$ (CGC97)
413	16	0045.5-7325	50.6	6.8	2.98e-02 ± 1.6e-03	0.020	SNR 0045-73.4 (WW92, RLG94) 13 cm
414	15	0044.7-7324	43.7	8.5	1.73e-02 ± 1.3e-03	0.007	SNR 0044-7325 (WW92, RLG94) 13 cm
419	16	0045.5-7325	88.2	4.7	3.72e-02 ± 1.5e-03	0.020	[SNR] 13 cm, part of source 413?
424	25	0050.0-7327	36.8	2.2	1.46e-02 ± 8.6e-04	0.011	[hard]
431	64	0116.1-7326	67.5	5.9	5.51e-03 ± 5.5e-04	0.005	[stellar] GSC 9142.1764
434	18	0045.6-7329	37.8	4.0	1.41e-02 ± 9.6e-04	0.006	[hard]
437	22	0047.3-7330	2.4	4.7	1.77e-02 ± 1.1e-03	0.007	SNR 0047-73.5 (WW92, FPH00) 13 cm
453	29	0050.3-7335	36.0	1.9	2.15e-02 ± 1.0e-03	0.009	HMXB Be/X RXJ0052.1-7319, pulsar (LPM99, ISC99)
454	21	0046.6-7335	34.0	10.8	5.15e-03 ± 7.2e-04	0.004	SNR 0046-73.5 (WW92) 13 cm
461	24	0049.2-7337	26.1	2.0	1.41e-01 ± 2.7e-03	0.060	SNR 0049-73.6 (WW92, CSM97) 13 cm
478	65	0117.2-7341	16.2	0.8	1.11e-01 ± 1.8e-03	0.016	fg Star G5V, HD 8191 (WW92, CSM97)
480	14	0043.7-7343	65.9	16.7	1.19e-03 ± 1.6e-03	0.004	
482	63	0115.8-7342	15.9	0.6	5.82 ± 1.2e-02	0.069	HMXB supergiant SMC X-1, pulsar (WW92)
496	28	0050.1-7346	43.5	10.4	9.39e-03 ± 2.4e-03	0.010	[nonstar]
623	33	0051.4-7455	2.5	0.7	4.12 ± 8.4e-03	0.413	fg Star G3:V+, RSCVn type, HD 5303 (WW92), 13 cm

Notes to the remark column to this and following tables:
Abbreviations for references given in parenthesis are described in the literature list.
Unsecure identifications from positional uncertainty begin with ? in the remark.
Candidates from literature are marked with ? after source class name.
Abbreviations: GSC: HST guide star catalogue (Lasker et al. 1990); fg: foreground.

The majority of classified sources (Table 7) consists of AGN and AGN candidates (46). Six AGN were optically identified by Tinney et al. (1997) and we suggest 22 new candidates which have an unresolved radio counterpart (mainly at $\lambda = 13$ cm). We classify as AGN additional 12 sources with high X-ray to optical flux ratio which are located south of the main body of the SMC. Table 7 contains further six uncertain AGN candidates due to large position uncertainties. The highly extended source 385 is identified with a cluster of galaxies. Another 24 sources are identified (12) and classified (12) as foreground stars.

X-ray sources intrinsic to the SMC are HMXBs, SSSs and SNRs. Fifteen HMXB and candidates, mainly X-ray pulsars discovered with instruments sensitive at energies of $1 - 10$ keV are included. Only three pulsars compiled in Table 4 of KPFH99 (namely AX J0051-722, XTE J0054-720 and XTE J0111.2-7317) were not detected in PSPC data. We note that source 79 in KPFH99

Table 4. PSPC sources detected in the ROSAT all-sky survey

1	2	3	4	5	6	7	8
No	BSC name 1RXS	d [″]	r_{90} [″]	$r_{\rm BSC}$ [″]	PSPC Count Rate [cts s^{-1}]	BSC Rate [cts s^{-1}]	Remarks
8	1RXS J005052.4-710914	10.5	20.2	11	2.04e-01 ± 1.1e-02	1.20e-01 ± 2.3e-02	fg Star F5V, HD 5028 (WW92)
47	1RXS J005837.9-713542	8.8	1.3	9	3.68e-01 ± 4.9e-03	2.81e-01 ± 3.2e-02	SSS 1E0056.8-7154, PN LIN333 (KP96)
52	1RXS J003704.1-713821	34.1	17.5	19	3.86e-02 ± 2.8e-03	5.71e-02 ± 1.4e-02	AGN? [hard] [nonstar] Radio SMC B0034-7155 (FJW97) 13 cm jets
107	1RXS J010403.5-720158	11.2	0.7	7	2.24 ± 2.1e-02	2.02 ± 7.7e-02	SNR 0102-72.3 (WW92, FPW99) 13 cm
176	1RXS J003723.2-721415	14.0	1.2	8	4.40e-01 ± 5.4e-03	3.49e-01 ± 3.0e-02	SSS 1E0035.4-7230 (KP96)
217	1RXS J010500.1-722305	17.5	2.1	11	3.12e-01 ± 4.6e-03	2.36e-01 ± 2.8e-02	SNR 0103-72.6 (WW92, CSM97) 13 cm
461	1RXS J005108.0-732134	9.8	2.0	21	1.41e-01 ± 2.7e-03	8.08e-02 ± 1.6e-02	SNR 0049-73.6 (WW92, CSM97) 13 cm
478	1RXS J011836.8-732529	6.2	0.8	14	1.11e-01 ± 1.8e-03	6.45e-02 ± 1.8e-02	fg Star G5V, HD 8191 (WW92, CSM97)
482	1RXS J011705.9-732632	1.5	0.6	8	5.82 ± 1.2e-02	7.20e-01 ± 6.4e-02	HMXB supergiant SMC X-1, pulsar (WW92)
512	1RXS J004820.7-733154	14.9	24.1	8	8.10e-03 ± 2.5e-03	1.99e-01 ± 2.2e-02	SSS RXJ0048.4-7332, symbiotic star M0 (KP96, M92)
621	1RXS J004402.7-743737	6.1	5.9	10	8.96e-02 ± 1.6e-03	6.51e-02 ± 1.3e-02	[fg Star] GSC 9141.1004
623	1RXS J005307.5-743903	2.4	0.7	6	4.12 ± 8.4e-03	2.38 ± 6.3e-02	fg Star G3:V+, RSCVn type, HD 5303 (WW92), 13 cm
683	1RXS J012522.3-750015	2.1	10.2	12	6.26e-02 ± 5.2e-03	6.42e-02 ± 1.3e-02	fg Star SAO 255776 (SIM)
709	1RXS J005655.1-751349	2.6	4.3	7	2.13e-01 ± 2.4e-03	3.00e-01 ± 2.4e-02	[AGN] GSC 9142.0531
721	1RXS J012254.1-752117	10.2	1.4	9	8.15e-01 ± 1.2e-02	5.28e-01 ± 6.7e-02	fg Star WD, FAUST 199 (SIM)
734	1RXS J013114.0-755643	15.0	17.7	7	2.28e-01 ± 9.7e-03	2.27e-01 ± 2.0e-02	fg Star K0, CD-76 56 (SIM)

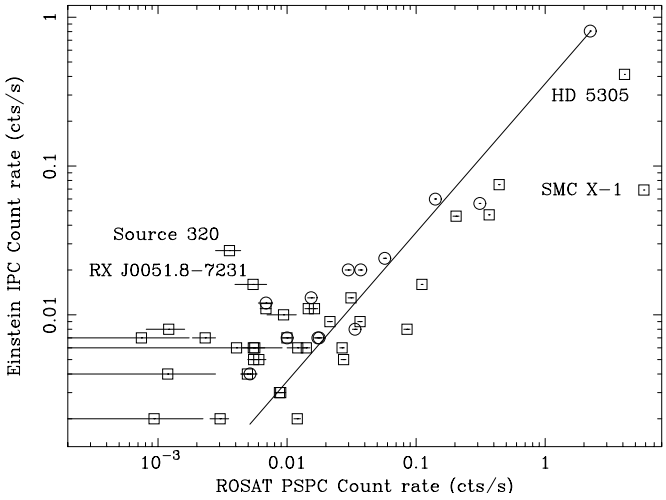

Fig. 4. Einstein IPC vs. ROSAT PSPC count rates. Sources identified with SNRs are marked with circles. The line is a linear fit to the SNR data points

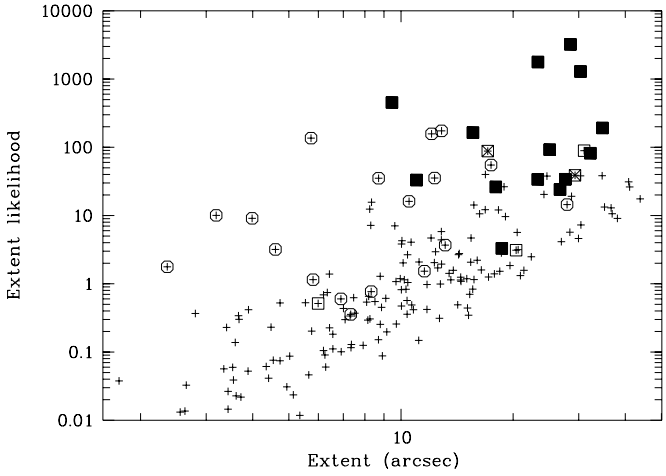

Fig. 5. Source extent and extent likelihood for the SMC PSPC sources with off-axis angle less than 18′ (plus signs). SNRs are marked with squares (filled: secure, open: candidates, crossed: classified in this work) and known point sources (X-ray binaries, SSSs, stars and AGN) with hexagons

(source 188 in Table 7) is probably not associated with AX J0051-722 because of the large (3′) offset in position. Most of the X-ray binary systems were detected with PSPC count rates between 2.7 10^{-3} cts s^{-1} and 8.9 10^{-2} cts s^{-1} which converts to X-ray luminosities between 4.5 10^{34} erg s^{-1} and 1.5 10^{36} erg s^{-1} (using a typical conversion factor of 1.67 10^{37} erg s^{-1}/cts s^{-1}; Kahabka & Pietsch 1996, hereafter KP96). This "quiescent" level is similar to that seen from persistent galactic high mass X-ray binaries like e.g. X Persei, RX J0146.9-6121 or RX J1037.5-5647 (Haberl et al. 1998; Reig & Roche 1999). With the exception of SMC X-1 and the peculiar soft X-ray pulsar RX J0059.2-7138 no other X-ray binary was found with a luminosity in excess of 10^{38} erg s^{-1} in the ROSAT band (0.1 − 2.4 keV). This casts doubt on earlier suggestions made before the launch of ROSAT (when only few X-ray binary systems were known in the MCs) that the fraction of high luminosity sources emitting near the Eddington limit in the MCs is higher than in the galactic population (Pakull 1989).

Four sources were earlier identified as SSSs, two were suggested by KP96 and three more are classified here as SSSs. Source 691 is likely identified with the SMC symbiotic star LIN 358 and is located together with source 664 remarkably far south of the SMC main body. Source 16 as third classified SSS is found north of the main body of the SMC.

Table 5. PSPC sources from the catalogue of Kahabka et al. (1999) not detected in the present analysis

KPFH99 No	Name	Comment[1]
6	0035.0-7354	D
14	0036.0-7210	$ML_{exi} = 11$
24	0038.0-7344	$ML_{exi} = 14$
25	0038.0-7327	near WSS, may be real
38	0042.2-7338	D
60	0047.5-7308	two catalogue sources (413/419)
73	0050.7-7226	D
75	0050.8-7341	WSS, not real
81	0051.7-7341	$ML_{exi} = 10$
90	0053.0-7239	$ML_{exi} = 10$
91	0053.1-7311	$ML_{exi} = 11$
97	0053.8-7252	$ML_{exi} = 11$
99	0054.3-7330	$ML_{exi} = 11$
112	0055.9-7257	D
113	0056.4-7159	D
119	0057.2-7156	$ML_{exi} = 13$
132	0058.5-7249	D
136	0058.9-7255	D
142	0059.7-7148	$ML_{exi} = 12$
156	0101.0-7151	$ML_{exi} = 11$
157	0101.0-7211	D
161	0101.3-7118	D
165	0101.8-7249	WSS, not real
167	0101.8-7233	$ML_{exi} = 14$
168	0102.1-7236	D
172	0102.8-7216	D
173	0102.9-7111	D
185	0104.2-7102	WSS, not real
186	0104.7-7203	near WSS, may be real
190	0105.3-7126	$ML_{exi} = 14$
192	0105.4-7219	$ML_{exi} = 11$
197	0106.3-7125	D
207	0108.5-7247	$ML_{exi} = 12$
210	0109.0-7243	$ML_{exi} = 13$
213	0109.5-7226	$ML_{exi} = 10$
215	0110.6-7217	$ML_{exi} = 12$
223	0112.7-7207	not real, largest extent in KPFH99
241	0116.8-7314	D
243	0117.2-7238	D

[1] Artifacts marked as D by KPFH99; likelihood of existence ML_{exi} from KPFH99.

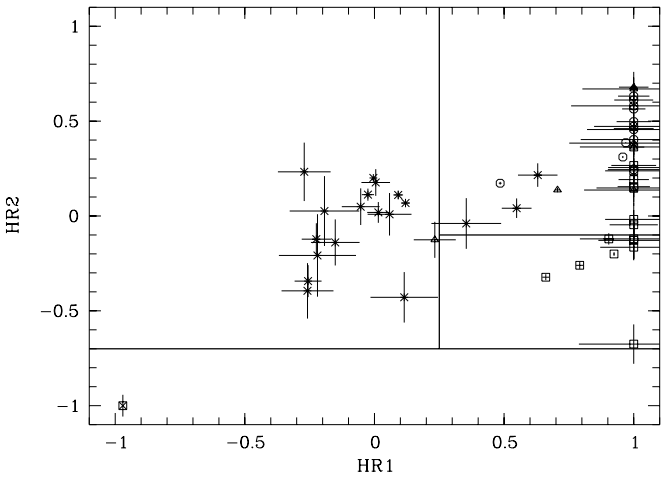

Fig. 6. Hardness ratios of identified and classified PSPC sources in the SMC area. X-ray binaries are marked with a hexagon, SSSs with crossed square, SNRs with square, stars with ×, and AGN with triangle. The thick lines separate areas where only members of a single class were found in the LMC (HP99). Only sources with error on HR1 and HR2 less than 0.25 are shown

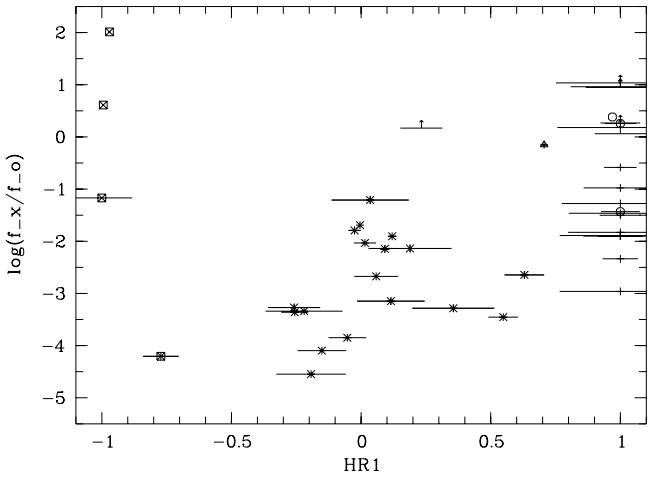

Fig. 7. Flux ratio f_x/f_{opt} as function of hardness ratio 1 (HR1). The optically identified sources are marked with different symbols (X-ray binaries: hexagon, SSSs: crossed square, foreground stars: × and AGN: triangle). Unidentified sources with error on HR1 less than 0.25 and nearby GSC entry are shown with HR1 error bars. Some lower limits derived from the optically brightest objects in the error circle are indicated by arrows

SNRs form the largest group of the SMC sources in Table 7. However, it should be noted that the class of SNRs is more complete than the class of X-ray binaries because the latter can not be uniquely separated from the hard sources. Fourteen clearly extended X-ray sources are identified with known SNRs and three with new candidates from radio investigations. In the work here another two sources are classified as SNR, both significantly extended X-ray sources. SNR 0102-72.3 (source 107) is by far the brightest in this sample of SNRs and amounts to about 75% of the total known SNR X-ray luminosity in the SMC of $\sim 5\ 10^{37}$ erg s^{-1} (using the same count rate conversion factor from above).

The classification of sources as [hard], [nonstar] and [stellar] does not allow a unique identification of the origin of the X-ray emission but restricts the number of possibilities. [Hard] and [nonstar] objects are likely candidates for X-ray binaries or background AGN while the [stellar] classification most likely selects foreground stars, but bright SMC stars can not be excluded as e.g. the Be X-ray binaries show typical optical magnitudes of 15 (cf. HP99).

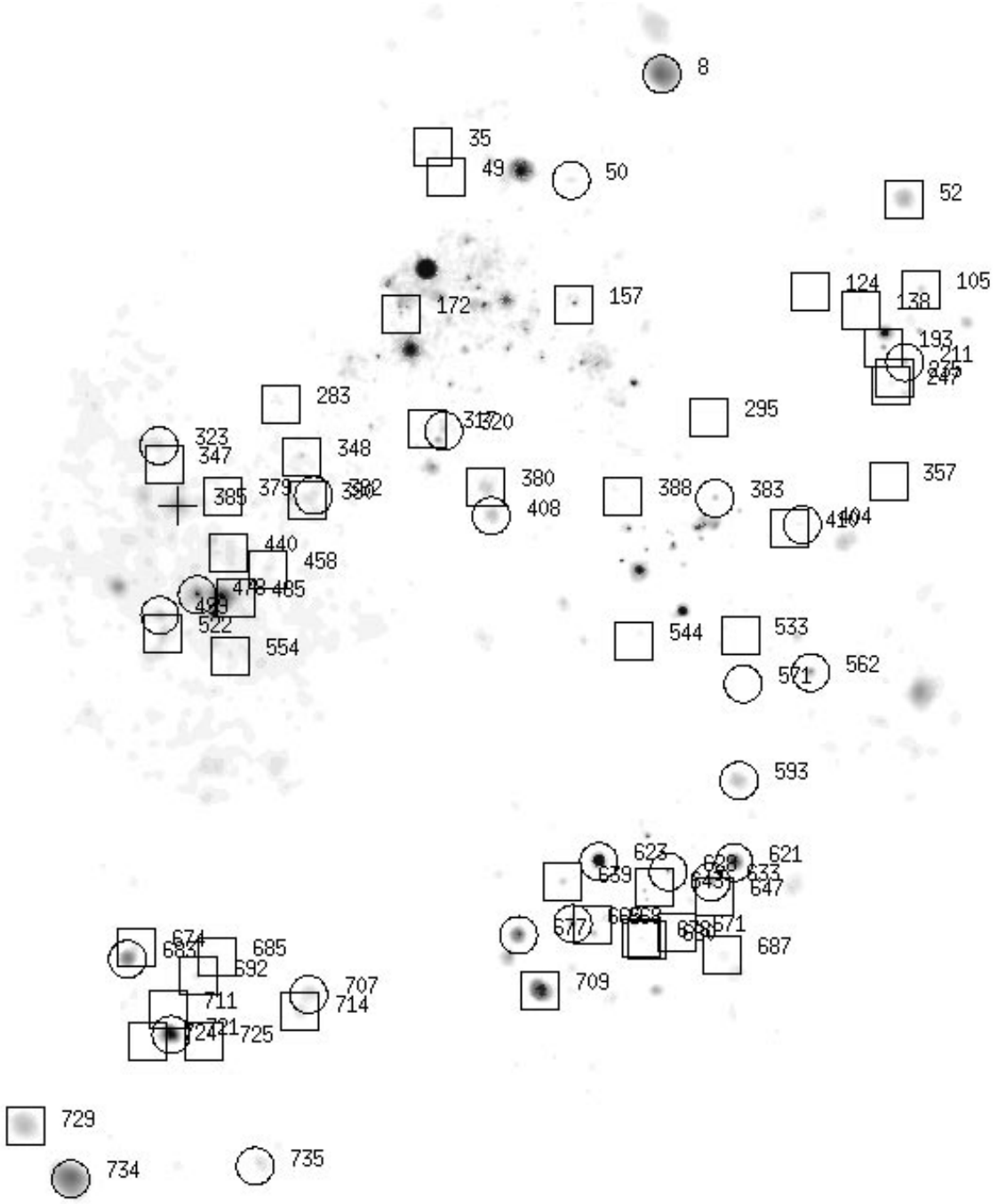

Fig. 8. Distribution of foreground and background objects in the SMC region detected with the ROSAT PSPC. Foreground stars and candidates are marked with circle, AGN and AGN candidates with squares. The only source (385) identified with a cluster of galaxies is marked by a plus. Source numbers refer to Table 7

3.3. Radio sources

Besides the radio catalogues covered by SIMBAD we correlated the PSPC catalogue with a preliminary list of radio sources resulting from the ATCA mosaic high resolution survey (Filipović & Stavely-Smith, in preparation). The PSPC sources detected at $\lambda = 13$ cm ($\nu = 2.37$ GHz) are indicated by "13 cm" in the comment column of Table 7. An inspection of the source morphologies on the 13 cm image revealed many point sources which are candidates for background AGN. In three cases jet like structures indicate radio lobes (sources 52, 157 and 390). Most known SNRs and SNR candidates are detected in the ATCA $\lambda = 13$ cm image and a new candidate (source 448) is found in the Eastern Wing of the SMC.

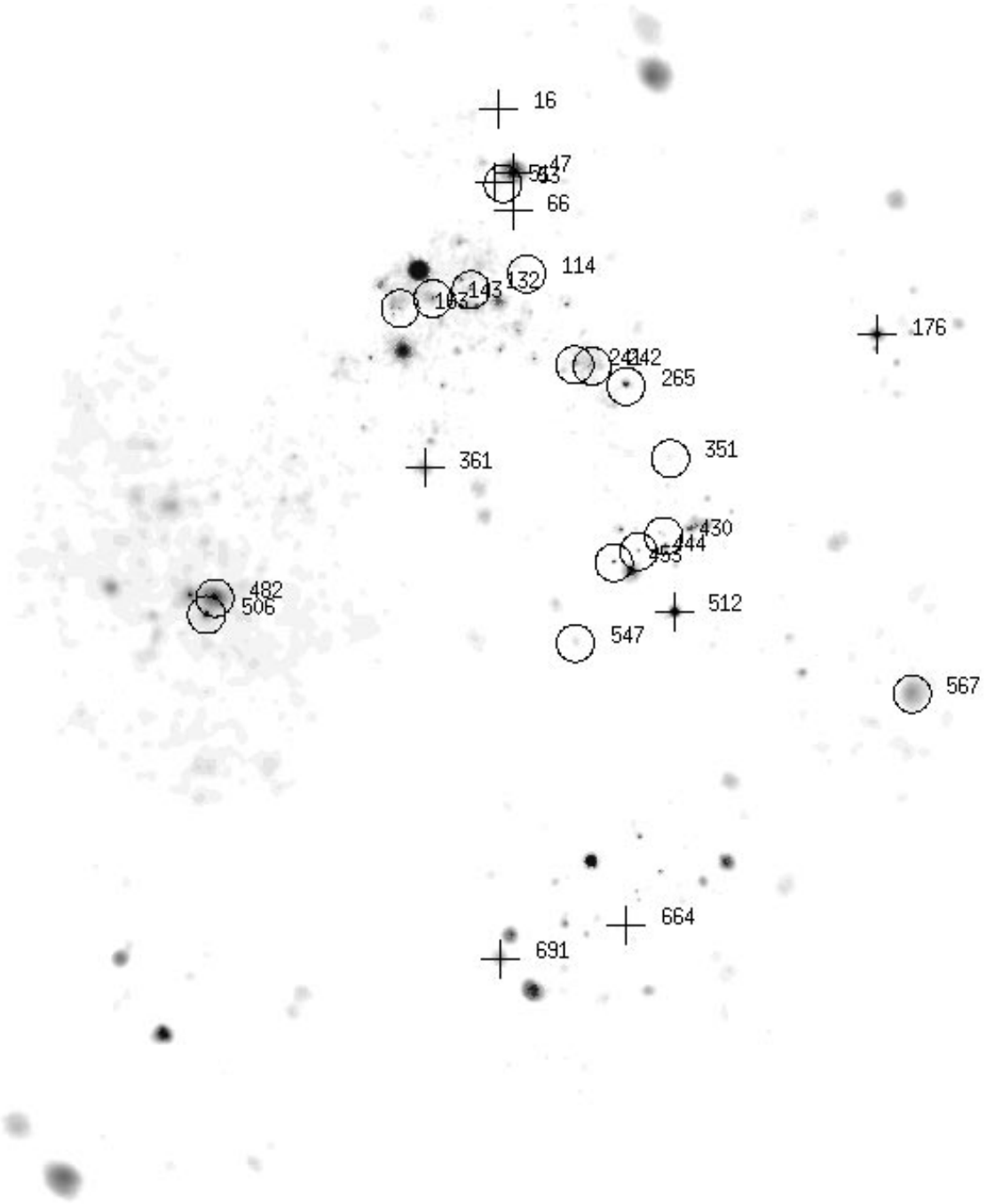

Fig. 9. Distribution of SSS (plus) and X-ray binaries (circle) including new candidates from this work

3.4. Spatial distribution of source populations

The spatial distribution of the different identified (including elsewhere published candidates) and classified PSPC sources from our SMC catalogue is shown in Figs. 8-10. Foreground stars and AGN are found in the whole field covered by PSPC observations (Fig. 8). Although, a lower density of detected AGN is expected along the main body of the SMC due to absorption of the X-ray emission, the small number of background objects in that area seen in Fig. 8 is mainly caused by incomplete classification of hard X-ray sources. The SMC intrinsic sources like HMXBs and SNRs are preferentially distributed along the main body of the SMC (Figs. 9 and 10). The high density might be caused by projection of a more extended distribution as Cepheid distances indicate a depth of the SMC of about 20 kpc (Mathewson et al. 1988). SSSs are detected around the main body (Fig. 9), very similar to the LMC where the SSSs are only found around the optical bar (HP99). SSSs may also exist inside the main SMC body but their

Fig. 10. Distribution of SNRs and SNR candidates in the SMC

supersoft X-ray emission is absorbed by the dense gas and dust.

4. Summary

We analyzed the complete ROSAT PSPC pointed data covering the MCs to obtain a comprehensive overview of the X-ray source content of these nearby galaxies. The source catalogue of the LMC was published by Haberl & Pietsch (1999) and in the current work a complementary catalogue of 517 discrete sources in the SMC is presented. About 30% of the PSPC sources are identified with known sources or at least classified as candidates for AGN, foreground stars, SSSs or SNRs. A high fraction of AGN and AGN candidates was found mainly from comparison with available radio data. These samples of different source classes allow to investigate their properties on a large statistical basis in a galaxy as a whole, but further identification work is required to confirm the classification and further enlarge the samples.

Table 6. Classification criteria

Source class	selection	unidentified	classified sources
SSS	HR1+EHR1 < -0.70	3	3
fg star	HR1+EHR1 <0.25, HR2 $-$ EHR2 > -0.70	7	
	HR1 <0.25, HR2 > -0.70, EHR1 <0.25, EHR2 <0.25	1	
	EHR1 <0.25, $-0.75 <$HR1 <0.25, $\log(f_x/f_{opt}) < -0.5$	2	
	EHR1 <0.25, $0.25 <$HR1 <0.75, $\log(f_x/f_{opt}) < -1.0$	3	12
SNR	$ML_{ext} >50$, offaxis angle $<18'$	1	
	HR1 $-$ R1 >0.25, HR2 $-$ EHR2 > -0.70, HR2+EHR2 < -0.10	1	
	HR1 >0.25, $-0.70 <$HR2 < -0.10, EHR1 <0.25, EHR2 <0.25	0	2
hard	HR1 $-$ EHR1>0.75, HR2 $-$ EHR2 > -0.10	25	
	HR1 >0.75, HR2 > -0.10, EHR1 <0.25, EHR2 <0.25	1	26
AGN	EHR1 <0.25, HR1 >0.25, $\log(f_x/f_{opt}) > -1.0$	1	
	nonstar south of $-74^\circ\ 30'$	12	13
stellar	$r_{90} <20''$, distance to GSC entry $<r_{90}$	16	9
nonstar	lower limit of $\log(f_x/f_{opt})>0.0$	31	31

Acknowledgements. The ROSAT project is supported by the German Bundesministerium für Bildung und Forschung (BMBF/DLR) and the Max-Planck-Gesellschaft. This research has made extensive use of the SIMBAD data base operated at CDS, Strasbourg, France. For the presentation of Fig. 1 we used the Karma software package developed at ATNF.

References

Bickert K.F., Greiner J., Stencel R.E., 1996, LNP 472, Supersoft X-ray Sources, Greiner J. (ed.), p. 225 (BGS96)
Clark G.W., Remillard R.A., Woo J.W., 1997, ApJ 474, L111 (CRW97)
Coe M.J., Orosz J.A., 1999, MNRAS (in press) astro-ph/9908303, (CO99)
Corbet R., Marshall F.E., Lochner J.C., Ozaki M., Ueda Y., 1997, IAU Circ. 6803 (CML98)
Cowley A.P., Schmidtke P.C., McGrath T.K., Ponder A.L., Fertig R.M., 1997, PASP 109, 21 (CSM97)
Crampton D., Gussie G., Cowley A.P., Schmidtke P.C., 1997, AJ 114, 2353 (CGC97)
Filipović M.D., Jones P.A., White G.L., Haynes R.F., Klein U., Wielebinski R., 1997, A&AS 121, 321 (FJW97)
Filipović M.D., Haberl F., Pietsch W., Morgan D., 2000, A&A (submitted) (FHP00)
Filipović M.D., Haynes R.F., White G.L., Jones P.A., 1998, A&AS 130, 421 (FHW98)
Filipović M.D., Pietsch W., Haberl F., 2000, A&A (submitted) (FPH00)
Filipović M.D., Pietsch W., Haynes R.F., et al., 1998, A&AS 127, 119 (FPH98)
Filipović M.D., Pietsch W., White G.L., Haberl F., Stavely-Smith L., Jones P.A., Haynes R.F., Sasaki M., 1999, IAU Symp. 192, 104 (FPW99)
Haberl F., Angelini L., Motch C., White N.E., 1998, A&A 330, 189
Haberl F., Pietsch W., 1999, A&AS 139, 277 (HP99)
Hughes J.P., 1994, ApJ 427, L25 (H94)
Hughes J.P., Smith R.C., 1994, AJ 107, 1363 (HS94)
Imanishi K., Yogokawa J., Koyama K., 1998, IAU Circ. 7040 (IYK98)
Israel G.L., Stella L., Angelini L., et al., 1997, ApJ 484, L141 (ISA97)
Israel G.L., Stella L., Campana S., Covino S., Ricci D., Oosterbroek T., 1998, IAU Circ. 6999 (ISC98)
Israel G.L., Stella L., Covino S., Campana S., Mereghetti S., 1999, IAU Circ. 7101 (ISC99)
Kahabka P., Pietsch W., Hasinger G., 1994, A&A 288, 538
Kahabka P., Pietsch W., 1996, A&A 312, 919 (KP96)
Kahabka P., Pietsch W., 1998, IAU Circ. 6840 (KP98)
Kahabka P., Pietsch W., Filipović M.D., Haberl F., 1999, A&AS 136, 1 (KPFH99)
Lamb R.C., Prince T.A., Macomb D.J., Finger M.H., 1999, IAU Circ. 7081 (LPM99)
Lasker B.M., Sturch C.R., McLean B.J., Russel J.L., Jenkner H., Shara M.M., 1990, AJ 99, 2019
Macomb D.J., Finger M.H., Harmon B.A., Lamb R.C., Prince T.A., 1999, ApJ 518, L99 (MFH99)
Marshall F.E., Lochner J.C., 1998, IAU Circ. 6818 (ML98)
Mathewson D.S., Ford V.L., Visvanathan N., 1988, ApJ 333, 617
Pakull M., 1989, in Recent Developments of Magellanic Cloud Research, Boer K.S., Spite F., Stasinska G. (eds.). Paris: Observatoire de Paris, p. 183
Pfeffermann E., Briel U.G., Hippmann H., et al., 1986, Proc. SPIE 733, 519
Reig P., Roche P., 1999, MNRAS 306, 100
Rosado M., Le Coarer E., Georgelin Y.P., 1994, A&A 286, 231 (RLG94)
Santangelo A., Cusumano G., Israel G.L., et al., 1998, IAU Circ. 6818 (SCI98)
Schmidtke P.C., Cowley A.P., 1998, IAU Circ. 6880 (SC98)
Schmidtke P.C., Cowley A.P., Crane J.D., et al., 1999, AJ 117, 927 (SCC99)
Southwell K.A., Charles P.A., 1996, MNRAS 281, L63 (SC96)
Stevens J.B., Coe M.J., Buckley D.A.H., 1999, MNRAS 309, 421 (SCB99)
Tinney C.G., Da Costa G.S., Zinnecker H., 1997, MNRAS 285, 111 (TDZ97)

Trümper J., 1982, Adv. Space Res. 2, 241
Vogel M., Nussbaumer H., 1995, A&A 301, 170 (VN95)
Voges W., Aschenbach B., Boller Th., et al., 1996, IAU Circ. 6420
Voges W., Aschenbach B., Boller Th., et al., 1999, A&A 349, 389
Wang Q., Hamilton T.T., Helfand D.J., Wu X., 1991, ApJ 374, 475
Wang Q., Wu X., 1992, ApJS 78, 391 (WW92)
Ye T., Turtle A.J., Kennicutt R.C. Jr., 1991, MNRAS 249, 722 (YTK91)
Yogokawa J., Koyama K., 1998, IAU Circ. 6853 (YK98a)
Yogokawa J., Koyama K., 1998, IAU Circ. 7028 (YK98b)
Yogokawa J., Koyama K., 1998, IAU Circ. 6835 (YK98c)
Zimmermann H.U., Becker W., Belloni T., Döbereiner S., Izzo C., Kahabka P., Schwentker O., 1994, EXSAS User's Guide, MPE report 257

Table 7. Identified and classified PSPC sources

1	2	3	4	5	6	7	8	9	10	11
No	ML_{exi}	RA (J2000.0)	Dec	r_{90} ["]	Count Rate [cts s^{-1}]	HR1	HR2	Extent ["]	ML_{ext}	Remarks
105	140.2	00 35 30.3	−72 01 34	7.9	7.27e-03 ± 9.0e-04	1.00 ± 0.62	0.38 ± 0.12	8.3	0.8	AGN z = 0.666 (TDZ97)
193	206.7	00 37 20.5	−72 18 01	4.3	7.49e-03 ± 8.1e-04	1.00 ± 1.09	−0.06 ± 0.12	0.5	0.0	AGN z = 0.922 (TDZ97)
235	47.6	00 36 34.1	−72 25 42	11.5	3.92e-03 ± 7.1e-04	1.00 ± 0.89	0.10 ± 0.18	11.6	1.5	AGN z = 1.220 (TDZ97)
247	82.2	00 36 41.3	−72 27 43	9.0	4.87e-03 ± 7.4e-04	1.00 ± 0.59	0.11 ± 0.15	7.3	0.4	AGN z = 1.624 (TDZ97)
283	64.6	01 12 48.6	−72 36 18	9.1	4.01e-03 ± 6.4e-04	1.00 ± 1.64	0.18 ± 0.16	0.0	0.0	AGN z = 1.376 (TDZ97)
379	97.7	01 16 34.1	−72 59 36	14.0	6.04e-03 ± 8.2e-04	1.00 ± 0.28	0.50 ± 0.10	27.9	14.5	AGN z = 0.253 (TDZ97)
35	12.1	01 03 32.4	−71 29 13	45.3	2.32e-03 ± 2.6e-03		1.00 ± 0.73	0.0	0.0	AGN? 13 cm
49	11.9	01 02 49.5	−71 37 09	42.6	3.41e-03 ± 4.4e-03	1.00 ± 0.84	−1.00 ± 1.69	0.0	0.0	AGN? 13 cm
52	326.6	00 36 56.9	−71 38 15	17.5	3.86e-02 ± 2.8e-03	1.00 ± 0.25	0.38 ± 0.06	51.3	19.1	AGN? [hard] [nonstar] Radio SMC B0034-7155 (FJW97) 13 cm jets
138	43.5	00 38 49.2	−72 08 32	8.4	2.60e-03 ± 5.6e-04	1.00 ± 0.97	0.26 ± 0.21	0.0	0.0	AGN? 13 cm
157	1632.9	00 55 27.2	−72 10 58	2.3	2.74e-02 ± 1.2e-03	1.00 ± 0.04	0.36 ± 0.04	8.2	12.4	AGN? Radio SMC B0053-7227 (FHW98) 13 cm jets
172	230.4	01 05 32.4	−72 13 31	4.2	7.34e-03 ± 7.1e-04	1.00 ± 0.37	0.46 ± 0.09	0.0	0.0	AGN? (FHP00) [nonstar] 13 cm
295	19.7	00 47 18.4	−72 39 42	49.8	4.06e-03 ± 5.1e-03	1.00 ± 0.82	1.00 ± 1.02	29.9	0.3	AGN? Radio SMC B0045-7255 (FHW98) 13 cm
317	34.9	01 04 07.4	−72 43 59	17.7	3.02e-03 ± 6.0e-04	1.00 ± 0.33	1.00 ± 0.89	28.7	19.1	AGN? 13 cm
388	16.5	00 52 18.9	−73 01 55	20.0	2.86e-03 ± 6.1e-04	1.00 ± 2.10	1.00 ± 3.41	15.0	1.2	AGN? 13 cm
390	57.5	01 11 33.6	−73 02 04	11.8	4.61e-03 ± 7.6e-04	1.00 ± 1.56	0.33 ± 0.15	12.8	1.9	AGN? Radio SMC B0110-7318 (FHW98) 13 cm jets
440	30.8	01 16 29.1	−73 15 00	11.9	1.97e-03 ± 4.0e-04	1.00 ± 1.13	1.00 ± 0.25	11.2	2.1	AGN? 13 cm
458	133.4	01 14 07.0	−73 20 04	6.8	3.79e-03 ± 4.7e-04	1.00 ± 0.20	0.67 ± 0.09	10.4	2.7	AGN? 13 cm [hard]
485	33.0	01 16 15.1	−73 26 57	13.0	1.32e-02 ± 8.6e-04	1.00 ± 0.06	0.68 ± 0.05	30.3	38.1	AGN? 13 cm [hard]
522	210.1	01 20 56.4	−73 34 51	8.7	8.54e-03 ± 7.9e-04	1.00 ± 0.10	0.26 ± 0.07	17.2	14.0	AGN? Radio SMC B0119-7350 (FHW98) [nonstar] 13 cm
533	13.9	00 44 38.0	−73 37 11	13.9	8.73e-04 ± 1.2e-03	1.00 ± 1.65	1.00 ± 0.79	2.7	0.0	AGN? 13 cm
544	10.8	00 51 15.3	−73 40 11	30.2	6.05e-03 ± 8.1e-03	1.00 ± 0.76	1.00 ± 1.58	12.7	0.3	AGN? Radio SMC B0049-7356 (FHW98) 13 cm
554	22.6	01 16 47.9	−73 42 30	20.1	1.80e-03 ± 1.7e-03	1.00 ± 0.47	1.00 ± 1.56	18.4	1.5	AGN? 13 cm
668	35.8	00 53 22.7	−74 56 03	11.5	1.14e-03 ± 2.5e-04	1.00 ± 0.91	0.22 ± 0.18	7.5	0.4	AGN? 13 cm
685	13.1	01 19 10.2	−75 01 46	52.1	1.02e-02 ± 1.2e-02			60.9	8.4	AGN? 13 cm
687	119.0	00 44 24.0	−75 02 30	24.1	5.46e-03 ± 2.1e-03	1.00 ± 0.08	0.46 ± 0.08	29.9	4.9	AGN? 13 cm [hard] [nonstar] [AGN]
692	35.7	01 20 36.0	−75 06 38	15.9	9.13e-03 ± 1.8e-03	1.00 ± 2.65	1.00 ± 1.50	10.4	0.4	AGN? SMC B0119-7522 (FHW98) 13 cm
711	21.7	01 22 54.4	−75 14 39	12.1	2.70e-03 ± 8.5e-04	1.00 ± 1.08	0.09 ± 0.33	0.0	0.0	AGN? Radio SMC B0121-7530 (FHW98)
639	243.9	00 55 31.2	−74 44 53	7.9	5.54e-03 ± 4.9e-04	1.00 ± 0.25	0.37 ± 0.07	20.2	17.1	[AGN] [nonstar]
643	77.1	00 49 15.2	−74 45 38	5.5	1.47e-03 ± 2.3e-04	1.00 ± 0.80	0.40 ± 0.14	0.0	0.0	[AGN] [nonstar]
647	47.2	00 45 10.8	−74 46 49	18.6	9.82e-03 ± 1.3e-03	1.00 ± 0.19	0.14 ± 0.08	17.4	1.0	[AGN] [nonstar] [hard]
671	29.2	00 47 39.0	−74 56 59	14.3	1.14e-03 ± 3.1e-04	1.00 ± 0.99	1.00 ± 1.52	10.4	0.6	[AGN] [nonstar]
674	30.9	01 24 36.7	−74 57 15	27.5	1.12e-02 ± 2.4e-03	1.00 ± 2.00	−0.25 ± 0.21	0.0	0.0	[AGN] [nonstar]
678	49.9	00 50 05.1	−74 59 08	10.3	1.28e-03 ± 2.6e-04	1.00 ± 0.68	−0.33 ± 0.15	5.0	0.1	[AGN] [nonstar]
680	12.4	00 49 36.4	−74 59 38	19.1	9.88e-04 ± 2.7e-04	1.00 ± 3.48		4.1	0.0	[AGN] [nonstar]
709	9072.8	00 56 55.5	−75 13 47	4.3	2.13e-01 ± 2.4e-03	0.71 ± 0.01	0.14 ± 0.01	36.8	104.8	[AGN] GSC 9142.0531
714	44.8	01 13 43.9	−75 17 60	43.8	2.60e-02 ± 4.3e-03	1.00 ± 0.53	1.00 ± 0.62	47.5	1.8	[AGN] [nonstar]
724	23.4	01 24 29.7	−75 22 43	11.9	3.16e-03 ± 9.4e-04	1.00 ± 1.09	1.00 ± 1.18	0.0	0.0	[AGN] [nonstar]
725	23.6	01 20 35.6	−75 24 10	11.8	2.90e-03 ± 9.1e-04	1.00 ± 1.01	1.00 ± 1.40	0.0	0.0	[AGN] [nonstar]
729	201.0	01 33 51.2	−75 41 10	36.5	7.61e-02 ± 7.3e-03	1.00 ± 0.87	0.10 ± 0.09	82.1	10.2	[AGN] [nonstar]
124	17.3	00 41 50.7	−72 04 43	44.8	3.46e-03 ± 3.4e-03	1.00 ± 0.50	1.00 ± 3.23	36.2	0.6	? AGN? Radio SMC B0040-7220 (FJW97) 13 cm
347	14.4	01 20 02.1	−72 49 58	62.1	2.59e-03 ± 1.9e-03	1.00 ± 0.47	1.00 ± 0.85	0.0	0.0	? AGN? 13 cm
348	278.9	01 11 40.9	−72 50 28	4.1	6.95e-03 ± 6.8e-04	1.00 ± 0.30	0.53 ± 0.09	3.4	0.2	? AGN z = 0.197 (TDZ97)
357	28.2	00 36 18.8	−72 53 00	61.8	1.39e-02 ± 3.2e-03	1.00 ± 0.62	1.00 ± 0.90	53.6	0.9	? AGN? Radio SMC B0033-7309 (FHW98) 13 cm
380	91.8	01 00 38.5	−72 59 51	24.9	2.29e-02 ± 2.0e-03	0.23 ± 0.08	−0.13 ± 0.10	55.4	16.9	? AGN? 13 cm [nonstar]
410	35.1	00 41 58.9	−73 07 53	45.1	7.79e-03 ± 1.3e-03	1.00 ± 0.25	0.45 ± 0.13	63.3	8.1	? AGN Radio SMC B0040-7323 (FHW98) 13 cm
385	604.8	01 19 25.4	−73 01 29	13.2	3.13e-02 ± 1.6e-03	1.00 ± 0.08	0.59 ± 0.03	71.3	227.9	Cluster z = 0.0656 (CGC97)
8	378.5	00 50 54.5	−71 09 12	20.2	2.04e-01 ± 1.1e-02	−0.26 ± 0.05	−0.34 ± 0.08	43.3	3.2	fg Star F5V, HD 5028 (WW92)
50	47.1	00 55 47.3	−71 38 03	10.0	4.90e-03 ± 7.4e-04	−0.22 ± 0.15	−0.21 ± 0.22	0.0	0.0	fg Star F5/F6V, HD 5572 (SIM)
323	35.2	01 20 14.1	−72 45 04	28.1	9.10e-03 ± 1.3e-03	−0.19 ± 0.13	0.03 ± 0.18	8.0	0.0	fg Star A9/F0, HD 8353 (SIM)
478	9966.1	01 18 38.0	−73 25 26	0.8	1.11e-01 ± 1.8e-03	0.12 ± 0.02	0.07 ± 0.02	4.0	9.1	fg Star G5V, HD 8191 (WW92,CSM97)
562	298.3	00 40 00.9	−73 45 42	5.1	1.66e-02 ± 1.2e-03	−0.05 ± 0.07	0.05 ± 0.10	6.9	0.6	fg Star F3V, HD 3880 (SIM)
571	19.4	00 44 14.7	−73 50 05	13.8	2.05e-03 ± 5.4e-04	1.00 ± 2.22	1.00 ± 2.93	0.0	0.0	fg Star F0V, HD 4319 (SIM)

Table 7. continued

1	2	3	4	5	6	7	8	9	10	11
No	ML_{exi}	RA (J2000.0)	Dec	r_{90} [']	Count Rate [cts s^{-1}]	HR1	HR2	Extent [']	ML_{ext}	Remarks
593	74.9	00 44 05.1	−74 15 49	27.6	2.04e-02 ± 2.0e-03	−0.15 ± 0.09	−0.14 ± 0.12	0.0	0.0	fg Star F6IV/V, HD 4309 (SIM)
623	30216.	00 53 07.3	−74 39 05	0.7	4.12 ± 8.4e-03	−0.00 ± 0.00	0.20 ± 0.00	2.4	1.8	fg Star G3:V+, RSCVn type, HD 5303 (WW92), 13 cm
633	652.3	00 45 31.7	−74 43 11	6.1	1.50e-02 ± 7.9e-04	0.55 ± 0.06	0.04 ± 0.05	22.4	30.8	fg Star F0V, HD 4512 (SIM)
683	242.2	01 25 21.7	−75 00 15	10.2	6.26e-02 ± 5.2e-03	0.06 ± 0.08	0.01 ± 0.11	21.7	8.1	fg Star SAO 255776 (SIM)
721	15275.	01 22 52.3	−75 21 25	1.4	8.15e-01 ± 1.2e-02	−0.99 ± 0.00	1.00 ± 1.47	8.7	35.2	fg Star WD, FAUST 199 (SIM)
734	683.0	01 31 10.8	−75 56 33	17.7	2.28e-01 ± 9.7e-03	0.01 ± 0.04	0.02 ± 0.05	60.7	12.0	fg Star K0, CD-76 56 (SIM)
211	143.6	00 36 01.9	−72 21 12	5.4	7.34e-03 ± 8.3e-04	0.35 ± 0.13	−0.04 ± 0.13	0.0	0.0	[fg Star]
320	18.9	01 03 08.4	−72 44 50	17.2	3.58e-03 ± 7.9e-04	0.36 ± 0.16	−1.00 ± 1.71	0.0	0.0	[fg Star] GSC 9141.7584
383	122.7	00 46 41.0	−73 01 14	6.4	7.18e-03 ± 7.5e-04	−0.26 ± 0.10	−0.39 ± 0.15	0.0	0.0	[fg Star] GSC 9141.7796
404	23.4	00 41 16.4	−73 06 41	35.6	5.75e-03 ± 1.0e-03	0.19 ± 0.16	1.00 ± 1.12	17.9	0.3	[fg Star] GSC 9141.4223?
408	61.1	01 00 19.3	−73 07 34	40.4	2.94e-02 ± 3.1e-03	−0.27 ± 0.10	0.23 ± 0.15	14.5	0.0	[fg Star]
499	98.4	01 21 04.1	−73 30 01	9.6	1.29e-02 ± 1.6e-03	0.11 ± 0.13	−0.43 ± 0.13	3.4	0.0	[fg Star] GSC 9142.2276
621	2256.4	00 44 04.0	−74 37 40	5.9	8.96e-02 ± 1.6e-03	0.09 ± 0.02	0.11 ± 0.02	41.1	156.0	[fg Star] GSC 9141.1004
628	594.4	00 48 26.2	−74 41 09	3.0	6.51e-03 ± 3.9e-04	0.63 ± 0.08	0.22 ± 0.06	3.7	0.3	[fg Star] GSC 9142.0870
665	355.6	00 54 46.1	−74 55 51	5.7	1.08e-02 ± 6.0e-04	0.00 ± 0.06	0.18 ± 0.07	16.3	10.6	[fg Star]
677	1634.0	00 58 28.6	−74 59 06	6.4	5.83e-02 ± 1.4e-03	−0.03 ± 0.02	0.11 ± 0.03	33.5	42.2	[fg Star] GSC 9141.7527
707	27.1	01 13 03.9	−75 13 33	59.8	3.11e-02 ± 4.7e-03	0.03 ± 0.15	1.00 ± 2.31	54.4	2.0	[fg Star] GSC 9347.0385?
735	86.7	01 17 39.9	−75 58 11	69.2	1.77e-01 ± 1.0e-02	−0.22 ± 0.06	−0.12 ± 0.08	167.6	41.2	[fg Star]
53	21306.	00 59 11.3	−71 38 45	2.8	8.38 ± 5.0e-02	0.48 ± 0.01	0.17 ± 0.01	16.0	14.5	HMXB Be/X RXJ0059.2-7138, soft pulsar (H94, SC96)
132	1670.4	01 01 01.1	−72 06 57	2.8	5.37e-02 ± 2.1e-03	1.00 ± 0.15	0.47 ± 0.04	12.3	35.4	HMXB Be/X RXJ0101.0-7206 (KP96, SCB99)
143	662.2	01 03 14.0	−72 09 16	3.4	1.54e-02 ± 9.6e-04	1.00 ± 0.10	0.24 ± 0.06	10.5	16.1	HMXB Be/X SAXJ0103.2-7209, pulsar (ISC98, HS94, CO99)
163	201.0	01 05 08.9	−72 11 44	6.6	6.86e-03 ± 6.7e-04	1.00 ± 0.20	0.40 ± 0.09	10.6	4.1	HMXB Be/X AXJ0105-722, pulsar (YK98b, FHP00)
241	1440.6	00 54 55.4	−72 26 46	3.5	3.68e-02 ± 1.5e-03	1.00 ± 0.04	0.56 ± 0.03	17.4	54.9	HMXB Be/X XTEJ0055-724, pulsar (ML98, SCI98, SCB99, CO99)
265	17.6	00 51 51.2	−72 32 07	45.8	5.45e-03 ± 1.5e-03	1.00 ± 0.71	1.00 ± 1.75	0.0	0.0	HMXB Be/X RXJ0051.8-7231, pulsar (WW92, ISA97, SCB99)
351	143.3	00 49 02.5	−72 50 52	13.7	6.42e-03 ± 8.7e-04	1.00 ± 0.24	1.00 ± 0.34	26.3	9.6	HMXB Be/X AXJ0049-729, pulsar (YK98c, KP98, SCB99, CO99)
427	107.5	00 49 29.6	−73 10 56	5.5	3.17e-03 ± 4.7e-04	1.00 ± 0.53	1.00 ± 0.20	4.7	0.5	HMXB Be/X AXJ0049-732, pulsar (IYK98, FPH00)
444	152.3	00 50 44.3	−73 15 58	4.9	4.52e-03 ± 5.5e-04	1.00 ± 0.24	0.58 ± 0.10	5.8	1.1	HMXB Be/X AXJ0051-73.3, pulsar (CSM97, YK98a, SC98, CO99)
453	1474.8	00 52 13.9	−73 19 13	1.9	2.15e-02 ± 1.0e-03	1.00 ± 0.07	0.61 ± 0.04	4.6	3.2	HMXB Be/X RXJ0052.1-7319, pulsar (LPM99, ISC99)
482	33862.	01 17 05.5	−73 26 32	0.6	5.82 ± 1.2e-02	0.97 ± 0.00	0.39 ± 0.00	5.7	136.1	HMXB supergiant SMC X-1, pulsar (WW92)
506	26511.	01 17 41.4	−73 30 49	0.6	9.65e-01 ± 5.3e-03	0.96 ± 0.00	0.31 ± 0.01	3.2	10.1	HMXB Be/X RXJ0117.6-7330, pulsar (MFH99, CRW97)
547	1107.7	00 54 30.8	−73 40 55	10.5	4.04e-01 ± 2.2e-02	1.00 ± 0.06	0.63 ± 0.04	36.4	23.6	HMXB Be/X SMC X-2
567	995.4	00 32 56.1	−73 48 19	12.9	8.88e-02 ± 4.0e-03	1.00 ± 0.07	0.50 ± 0.03	49.7	18.5	HMXB Be/X, 2 Be stars in error circle (KP96, SCB99)
114	74.1	00 57 48.4	−72 02 42	7.9	3.03e-03 ± 5.0e-04	1.00 ± 0.52	1.00 ± 0.35	0.0	0.0	HMXB? AXJ0058-72.0, pulsar (YK98a)
242	569.2	00 53 53.3	−72 27 01	25.7	8.50e-02 ± 4.7e-03	1.00 ± 0.18	0.46 ± 0.05	72.3	19.8	HMXB? XTEJ0053-724, pulsar (CML98)
47	14089.	00 58 37.2	−71 35 50	1.3	3.68e-01 ± 4.9e-03	−0.99 ± 0.00	−1.00 ± 0.26	12.8	174.1	SSS 1E0056.8-7154, PN LIN333 (KP96)
66	172.7	00 58 37.1	−71 46 02	8.1	2.71e-02 ± 2.7e-03	−1.00 ± 0.03		13.1	3.7	SSS RXJ0058.6-7146 (KP96)
176	15504.	00 37 20.2	−72 14 12	1.2	4.40e-01 ± 5.4e-03	−0.97 ± 0.00	−1.00 ± 0.06	12.1	157.4	SSS 1E0035.4-7230 (KP96)
512	17.9	00 48 23.1	−73 31 43	24.1	8.10e-03 ± 2.5e-03	−1.00 ± 0.24		0.0	0.0	SSS RXJ0048.4-7332, symbiotic star M0 (KP96, M92)
51	25.7	00 59 41.7	−71 38 15	14.5	2.94e-03 ± 6.1e-04	−1.00 ± 0.12		0.0	0.0	SSS? RXJ0059.6-7138, PN LIN357 (KPFH99)
361	134.8	01 03 52.1	−72 54 28	32.4	4.40e-02 ± 9.6e-03	−1.00 ± 0.10		63.7	5.1	SSS? RXJ0103.8-7254 (KP96)
16	15.6	00 59 26.3	−71 18 47	26.0	3.00e-03 ± 8.1e-04	−1.00 ± 0.16		15.1	0.4	[SSS]
664	46.3	00 50 35.0	−74 55 44	9.3	2.11e-03 ± 2.9e-04	−0.77 ± 0.07	−1.00 ± 0.69	0.0	0.0	[SSS]
691	258.9	00 59 10.6	−75 05 22	19.5	2.76e-02 ± 1.2e-03	−1.00 ± 0.05		0.0	0.0	[SSS] LIN358, symbiotic star (BGS96,VN95)
45	67.5	01 00 21.9	−71 33 28	13.0	8.38e-03 ± 1.1e-03	1.00 ± 0.14	−0.13 ± 0.10	32.2	81.9	SNR DEM S108 (FPH98) 13 cm
107	27963.	01 04 02.0	−72 01 48	0.7	2.24 ± 2.1e-02	0.92 ± 0.00	−0.20 ± 0.01	9.5	452.9	SNR 0102-72.3 (WW92, FPW99) 13 cm
125	789.8	01 06 14.3	−72 05 18	3.6	3.36e-02 ± 1.5e-03	1.00 ± 0.06	0.19 ± 0.04	15.6	164.2	SNR 0104-72.3 (WW92) 13 cm
145	37.9	01 05 23.2	−72 09 26	13.2	1.22e-02 ± 1.1e-03	1.00 ± 0.09	−0.05 ± 0.08	27.6	34.0	SNR DEM S128 (FPH98, FHP00) 13 cm
148	1272.5	00 59 25.4	−72 10 10	3.2	5.73e-02 ± 1.7e-03	0.90 ± 0.02	−0.12 ± 0.03	30.3	1289.2	SNR 0057-72.2 (YTK91,WW92) 13 cm
194	240.5	00 58 16.4	−72 18 05	6.5	1.00e-02 ± 7.2e-04	1.00 ± 0.14	0.15 ± 0.07	18.0	26.2	SNR 0056-72.5 (WW92) 13 cm
217	6323.8	01 05 03.5	−72 22 56	2.1	3.12e-01 ± 4.6e-03	0.66 ± 0.01	−0.32 ± 0.02	23.3	1775.3	SNR 0103-72.6 (WW92, CSM97) 13 cm
285	80.7	00 52 30.7	−72 37 24	12.7	6.86e-03 ± 8.7e-04	1.00 ± 0.33	−0.53 ± 0.10	26.7	24.0	SNR 0050-72.8 (WW92) 13 cm
401	23.4	00 47 31.3	−73 05 49	19.0	6.58e-03 ± 8.3e-04	1.00 ± 0.21	−0.68 ± 0.10	18.7	3.3	SNR 0045-7322 (RLG94) 13 cm
413	281.8	00 47 12.2	−73 08 26	6.8	2.98e-02 ± 1.6e-03	1.00 ± 0.11	0.24 ± 0.04	25.1	92.3	SNR 0045-73.4 (WW92, RLG94) 13 cm

Table 7. continued

1	2	3	4	5	6	7	8	9	10	11
No	ML_{exi}	RA (J2000.0)	Dec	r_{90} [']	Count Rate [cts s^{-1}]	HR1	HR2	Extent [']	ML_{ext}	Remarks
414	149.6	00 46 39.1	−73 08 39	8.5	1.73e-02 ± 1.3e-03	1.00 ± 0.13	−0.16 ± 0.06	34.7	191.9	SNR 0044-7325 (WW92,RLG94) 13 cm
437	451.4	00 49 06.9	−73 14 05	4.7	1.77e-02 ± 1.1e-03	1.00 ± 0.06	0.15 ± 0.06	11.0	33.1	SNR 0047-73.5 (WW92,FPH00) 13 cm
454	73.4	00 48 24.8	−73 19 24	10.8	5.15e-03 ± 7.2e-04	1.00 ± 0.21	0.36 ± 0.11	23.3	33.9	SNR 0046-73.5 (WW92) 13 cm
461	4781.7	00 51 06.5	−73 21 26	2.0	1.41e-01 ± 2.7e-03	0.79 ± 0.01	−0.26 ± 0.02	28.5	3218.9	SNR 0049-73.6 (WW92,CSM97) 13 cm
206	61.5	00 56 39.8	−72 20 28	7.4	2.42e-03 ± 4.1e-04	1.00 ± 0.55	1.00 ± 0.78	6.0	0.5	SNR? DEM S86 (FPH98) 13 cm
448	15.3	01 13 42.3	−73 17 17	22.9	1.43e-03 ± 1.7e-03	1.00 ± 0.74	1.00 ± 0.44	20.4	3.1	SNR? 13 cm, Radio SMC B0112-7333 (FJW97)
530	123.8	00 41 04.1	−73 36 39	11.0	9.50e-03 ± 9.3e-04	1.00 ± 0.11	−0.02 ± 0.09	31.0	89.1	SNR? DEM S5 (FPH98) 13 cm
137	26.5	01 04 17.4	−72 08 06	14.5	6.83e-03 ± 9.2e-04	1.00 ± 0.21	−0.12 ± 0.11	29.3	38.8	[SNR]
419	922.5	00 47 40.6	−73 09 30	4.7	3.72e-02 ± 1.5e-03	1.00 ± 0.09	0.27 ± 0.04	17.1	87.9	[SNR] 13 cm, part of source 413?
136	150.0	00 57 50.1	−72 07 56	5.1	8.82e-03 ± 1.2e-03	1.00 ± 0.22	0.58 ± 0.11	0.0	0.0	[hard]
160	213.2	01 05 35.0	−72 11 25	7.8	1.63e-02 ± 1.0e-03	1.00 ± 0.09	0.09 ± 0.06	16.8	40.0	[hard] associated with DEM S128? (FHP00)
162	1552.9	01 00 41.5	−72 11 34	2.3	2.67e-02 ± 1.1e-03	1.00 ± 0.07	0.33 ± 0.04	8.3	15.7	[hard] G star identification in SCC99 unlikely
170	243.6	00 57 31.8	−72 13 03	3.6	5.48e-03 ± 5.4e-04	1.00 ± 0.13	0.38 ± 0.09	3.9	0.4	[hard] [nonstar]
230	839.3	01 06 56.5	−72 24 52	2.4	1.20e-02 ± 7.1e-04	1.00 ± 0.13	0.43 ± 0.06	0.0	0.0	[hard]
232	161.7	01 08 35.4	−72 25 11	8.6	4.93e-03 ± 5.6e-04	1.00 ± 0.23	0.39 ± 0.10	19.1	9.6	[hard]
248	194.1	00 54 33.1	−72 28 08	45.7	9.18e-02 ± 7.7e-03	1.00 ± 0.12	0.20 ± 0.07	29.9	0.2	[hard]
249	38.7	00 55 34.2	−72 28 30	14.9	4.47e-03 ± 1.0e-03	1.00 ± 0.24	0.14 ± 0.19	13.6	1.1	[hard] [nonstar] 13 cm
253	75.0	01 09 01.2	−72 29 07	17.6	6.86e-03 ± 7.1e-04	1.00 ± 0.19	0.17 ± 0.09	40.8	31.2	[hard]
255	115.3	00 37 40.0	−72 29 35	8.7	5.46e-03 ± 8.0e-04	1.00 ± 0.20	0.28 ± 0.12	9.7	1.1	[hard]
368	103.4	01 18 55.4	−72 56 25	25.7	8.26e-03 ± 1.4e-03	1.00 ± 0.10	0.65 ± 0.04	53.0	14.2	[hard]
423	398.9	00 38 42.9	−73 10 21	16.1	3.35e-02 ± 2.2e-03	1.00 ± 0.14	0.39 ± 0.05	60.8	49.9	[hard] GSC 9141.4679
424	900.4	00 51 51.5	−73 10 31	2.2	1.46e-02 ± 8.6e-04	1.00 ± 0.08	0.36 ± 0.06	2.8	0.4	[hard]
434	583.6	00 47 23.4	−73 12 23	4.0	1.41e-02 ± 9.6e-04	1.00 ± 0.11	0.52 ± 0.06	9.6	7.1	[hard]
460	3202.0	01 23 27.2	−73 21 25	4.6	6.95e-02 ± 1.9e-03	1.00 ± 0.06	0.60 ± 0.02	32.9	143.1	[hard] GSC 9142.2001
590	122.1	01 14 21.3	−74 11 35	33.5	1.79e-02 ± 2.0e-03	1.00 ± 0.23	0.50 ± 0.11	42.9	1.1	[hard]
605	100.6	00 56 07.8	−74 30 12	15.8	4.13e-03 ± 4.9e-04	1.00 ± 0.23	−0.06 ± 0.09	27.3	6.1	[hard]
626	42.4	00 52 00.0	−74 40 21	16.5	2.20e-03 ± 2.6e-04	1.00 ± 0.21	1.00 ± 0.28	10.0	0.8	[hard]
694	181.5	00 43 31.5	−75 07 04	29.8	1.46e-02 ± 1.2e-03	1.00 ± 0.20	0.62 ± 0.05	54.0	16.4	[hard]
705	471.1	00 48 51.0	−75 12 56	9.7	1.17e-02 ± 7.7e-04	1.00 ± 0.24	0.31 ± 0.05	34.3	24.2	[hard]
708	86.9	00 54 43.9	−75 13 36	35.4	8.58e-03 ± 1.8e-03	1.00 ± 0.20	0.24 ± 0.10	0.0	0.0	[hard]
81	24.7	00 39 36.1	−71 53 09	25.3	7.54e-03 ± 1.7e-03	1.00 ± 1.13	0.16 ± 0.23	0.0	0.0	[nonstar]
103	10.1	01 00 34.4	−72 00 59	18.2	4.89e-03 ± 7.1e-03	1.00 ± 0.83		0.0	0.0	[nonstar]
130	17.1	00 34 50.3	−72 06 30	16.3	1.99e-03 ± 5.8e-04	1.00 ± 3.32	1.00 ± 1.76	6.3	0.1	[nonstar]
159	91.8	01 01 21.8	−72 11 19	9.8	1.51e-02 ± 2.2e-03	1.00 ± 0.98	1.00 ± 0.47	10.1	2.0	[nonstar]
177	18.0	01 00 46.8	−72 14 15	13.8	1.57e-03 ± 4.1e-04	1.00 ± 0.89	1.00 ± 0.98	8.1	0.5	[nonstar]
191	72.7	00 36 12.7	−72 17 45	6.7	3.68e-03 ± 6.1e-04	1.00 ± 0.76	0.10 ± 0.18	2.7	0.0	[nonstar]
282	15.7	01 07 48.9	−72 36 16	11.4	1.03e-03 ± 3.1e-04	1.00 ± 4.88	1.00 ± 2.22	0.0	0.0	[nonstar]
293	108.4	00 55 18.3	−72 38 56	5.6	4.24e-03 ± 6.2e-04	1.00 ± 0.54	1.00 ± 0.75	0.0	0.0	[nonstar] IRAS 00535-7254
313	329.8	01 07 29.0	−72 43 22	4.1	6.83e-03 ± 5.9e-04	1.00 ± 0.34	0.45 ± 0.08	0.0	0.0	[nonstar]
470	78.6	01 15 20.0	−73 23 51	6.3	2.67e-03 ± 3.8e-04	1.00 ± 0.53	0.35 ± 0.13	6.2	0.7	[nonstar]
472	10.1	00 51 07.5	−73 24 03	0.0	1.12e-03 ± 1.6e-03	1.00 ± 4.96		41.1	26.2	[nonstar]
496	39.7	00 52 02.5	−73 29 29	10.4	9.39e-03 ± 2.4e-03	1.00 ± 0.41	0.35 ± 0.25	3.9	0.1	[nonstar]
524	11.7	01 17 56.2	−73 35 19	13.1	8.34e-04 ± 1.1e-03	1.00 ± 1.55	1.00 ± 0.75	0.0	0.0	[nonstar]
204	32.0	01 00 11.5	−72 20 07	9.9	1.62e-03 ± 3.8e-04	1.00 ± 0.99	1.00 ± 0.58	0.0	0.0	[stellar] GSC 9138.1748
290	14.9	01 15 51.9	−72 37 51	18.4	9.55e-04 ± 1.5e-03	1.00 ± 1.10	1.00 ± 1.38	5.7	0.0	[stellar] GSC 9142.0918
303	43.7	01 13 03.4	−72 41 38	7.9	2.17e-03 ± 4.7e-04	1.00 ± 0.88	0.01 ± 0.20	0.0	0.0	[stellar] GSC 9142.2678
382	27.9	01 11 06.5	−73 00 58	14.3	4.17e-03 ± 7.6e-04	1.00 ± 4.58	−1.00 ± 1.04	0.0	0.0	[stellar] GSC 9142.2832, fg Star? (f_x/f_o)
431	178.6	01 17 28.7	−73 11 42	5.9	5.51e-03 ± 5.5e-04	1.00 ± 0.54	0.30 ± 0.09	10.0	3.8	[stellar] GSC 9142.1764
521	16.5	01 15 41.1	−73 34 49	12.1	1.49e-03 ± 3.4e-04	1.00 ± 2.62	−1.00 ± 1.60	0.0	0.0	[stellar] GSC 9142.2236
576	23.5	00 43 47.0	−73 55 19	18.7	3.23e-03 ± 7.0e-04	1.00 ± 1.99	1.00 ± 1.96	0.0	0.0	[stellar] GSC 9142.2186
618	35.7	00 50 05.9	−74 35 17	8.8	1.37e-03 ± 2.5e-04	1.00 ± 3.77	0.05 ± 0.18	0.0	0.0	[stellar] GSC 9142.0856
723	36.5	01 23 43.1	−75 21 47	9.2	5.43e-03 ± 1.2e-03	1.00 ± 2.01	1.00 ± 1.31	0.0	0.0	[stellar] GSC 9142.0956